Liquid Crystals
Publication details, including instructions for authors and subscription information:
http://www.informaworld.com/smpp/title~content=t713926090

Determination of symmetry and molecular arrangements of free-standing liquid crystal films using null-transmission ellipsometry

D. A. Olson; X. F. Han; P. M. Johnson; A. Cady; C. C. Huang

Online publication date: 11 November 2010

To cite this Article Olson, D. A. , Han, X. F. , Johnson, P. M. , Cady, A. and Huang, C. C.(2002) 'Determination of symmetry and molecular arrangements of free-standing liquid crystal films using null-transmission ellipsometry', Liquid Crystals, 29: 12, 1521 — 1528
To link to this Article: DOI: 10.1080/0267829021000017979
URL: http://dx.doi.org/10.1080/0267829021000017979

LIQUID CRYSTALS, 2002, VOL. 29, NO. 12, 1521–1528

Determination of symmetry and molecular arrangements of free-standing liquid crystal films using null-transmission ellipsometry

D. A. OLSON, X. F. HAN, P. M. JOHNSON, A. CADY and C. C. HUANG*

School of Physics and Astronomy, University of Minnesota, Minneapolis, Minnesota 55455, USA

(*Received 20 February 2002; accepted 21 May 2002*)

A high resolution null-transmission ellipsometry system has been developed for measurement of the optical properties of liquid crystal free-standing films. The ellipsometric parameters are measured to within a resolution of 0.002° from samples held in a sealed, temperature-controlled environment. By measuring the ellipsometric parameters as a function of applied electric field orientation, the optical symmetry and molecular orientations of free-standing liquid crystal films can be determined in some cases. Three carefully selected applications of this technique are presented.

1. Introduction

Liquid crystals with polar order are studied because many exhibit numerous mesophases and thus offer excellent systems for the study of phase transitions. Many recently synthesized liquid crystal materials have a large spontaneous polarization and exhibit phases showing ferroelectric, antiferroelectric, or ferrielectric responses to applied electric fields. Because these features allow for electro-optic switching, it is hoped that these compounds may be useful in high definition video displays and terabit/sec fibre-optic networking components. The identification and characterization of these phases are essential parts of this research. Many of these phases are smectic, i.e. they have a layered structure with no long range positional ordering within each layer. This makes it possible to create stable free-standing films.

In this paper a high resolution null-transmission ellipsometry system is presented which has been used to measure the optical properties of free-standing liquid crystal films. The application of an electric field in the plane of the film will align the net polarization in the film. This causes the c-director of the molecules to align due to the applied electric field because the net polarization of the film is related to the orientation of the molecules. Further, the dielectric tensor is also related to the orientation of the molecules. Therefore, by measuring the optical parameters as a function of the orientation of the applied electric field, the optical symmetry can be determined. Through simulation it is often also possible to determine the molecular orientation in these phases. A similar approach could be applied for studying films of solid material with no substrate. For most samples, they would need to be thin enough to have a measureable amount of transmission. The sample could be rotated mechanically or by an applied field for a specimen with a net in-plane polarization.

We begin with a description of the null-transmission ellipsometer. Following this, a method is described that is exploitable in most experiments—specifically when studying compounds exhibiting a smectic A (SmA) phase—for the measurement of several important parameters. Three key examples are presented which demonstrate the advantages of our null-transmission ellipsometry system.

*Author for correspondence;
e-mail: huang001@tc.umn.edu

2. Null-transmission ellipsometry design

Ellipsometry is a technique used to measure the effect that a sample has on polarized light [1]. Two measureable quantities that depend on the sample structure and orientation are (i) the amount that the polarization of the light is rotated by the sample and (ii) the phase lag the sample creates between the two orthogonal polarization components of the light. In a polarizer–compensator–sample–analyser null-transmission ellipsometry set-up, well-defined elliptically polarized light is transmitted through a film. A polarizer and analyser are then rotated to eliminate, or 'null', the transmitted light.

Before proceeding further it is useful to briefly describe free-standing liquid crystal films and how they are produced. Liquid crystal films are similar to soap bubbles

Liquid Crystals ISSN 0267-8292 print/ISSN 1366-5855 online © 2002 Taylor & Francis Ltd
http://www.tandf.co.uk/journals
DOI: 10.1080/0267829021000017979

in that they need no substrate. Unlike soap bubbles, free-standing liquid crystal films are stable in smectic phases and have a quantized number of layers. Our free-standing liquid crystal films are produced by pulling a sample across a hole in a glass cover slip using a glass spreader.

To describe the ellipsometric parameters it is necessary to define our coordinate system. p and s are the polarizations parallel and perpendicular to the plane of incidence of the beam travelling in the $\mathbf{k}$ direction, respectively (see figure 1). If we define unit vectors $\hat{\mathbf{p}}$, $\hat{\mathbf{s}}$, and $\hat{\mathbf{k}}$ along the p, s, k axes, respectively, then $\hat{\mathbf{p}} \times \hat{\mathbf{s}} = \hat{\mathbf{k}}$. The incidence plane here is defined by the incident and reflected beams, although the reflected beam is not measured. The $\hat{\mathbf{x}}$ axis, which is along the intersection of the film plane and the incidence plane, is also shown in figure 1. With those definitions the ellipsometric parameters (Δ and Ψ), are as follows: Δ is the necessary phase shift between the p- and s-components of the incident light for the transmitted light to be linearly polarized at an angle $\Psi + 90^\circ$ relative to the p-axis.

The components in our ellipsometry system are arranged as follows. The laser beam ($\lambda = 6328$ Å) is incident at 45° to the normal of the surface of the sample. Our system uses the window–polarizer–compensator–sample–analyser–window–detector (WPCSAWD) beam path, shown in figure 1. The incoming linearly polarizer laser light, chopped at 2033 Hz, passes through a 1/4 wave-plate with its fast axis aligned appropriately, so that circularly polarized light emerges. Thus the intensity

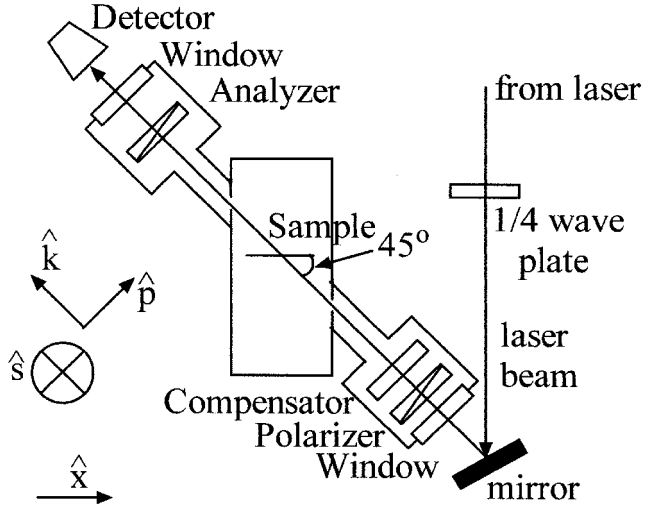

Figure 1. The null-transmission ellipsometry system, as described in detail in the text. The unit vector ($\hat{\mathbf{k}}$) which points along the direction of travel of the laser beam along with $\hat{\mathbf{p}}$ and $\hat{\mathbf{s}}$ which are parallel and perpendicular to the plane of incidence, respectively, are shown. The $\hat{\mathbf{x}}$ axis, which is along the intersection of the plane of the film and the incidence plane, is also shown.

after the polarizer is independent of the angle of the polarizer. The compensator is another 1/4 wave-plate with its fast axis fixed at -45° to the p axis. Positive angles are defined as clockwise rotations when looking along $\hat{\mathbf{k}}$. A current-to-voltage converter sends the signal from the detector to a lock-in amplifier and then a computer controlled data acquisition program.

The ellipsometric parameters, Δ and Ψ, are found by rotating the polarizer and analyser until a null signal is registered at the detector. With the configuration described above, the equations for Δ and Ψ are $\Delta = -2P_n + 90^\circ$ and $\Psi = A_n$, where P_n and A_n are the angles of the polarizer and analyser relative to the p axis that give zero transmitted intensity of the laser beam at the detector. [In our previous papers we used the incorrect equation $\Delta = -2P_n - 90^\circ$. This offsets all of our previously reported values of Δ by 180°, but does not change the values of any physical parameters reported.] P_n and A_n are found by fitting the transmitted intensity as a function of the polarizer angles to a quadratic equation and calculating the position of the minimum. Specifically, one of the polarizer angles is held fixed while the other rotates to find the orientation with minimum transmitted intensity for the rotating polarizer. This is then repeated for the other polarizer. This method works because the orientation of the polarizer giving minimum transmitted intensity does not strongly depend on the orientation of the analyser, and *vice-versa*. The polarizer and analyser are typically stepped through $\sim 1.400^\circ$ with steps of 0.200°. The procedure has a resolution of 0.002° in Δ and Ψ at a speed of one data point every 30 s. We have checked this resolution by studying very thin films, such as the study of the one-layer film presented in § 3.1.

The orientation of the transmission axes of the polarizer and analyser are set to a precision of 0.03° with respect to the optical table by insuring that the angle of linear polarization of the light after the polarizer does not change when the polarizer is rotated by 180° around the $\hat{\mathbf{p}}$ direction. The analyser is then set at $90 \pm 0.01^\circ$ to this angle. At this point the compensator is added to the system and is rotated until the light transmitted by it is linearly polarized when the polarizer is held at $-45 \pm 0.01^\circ$ to the p axis.

Up to now, more than three different optical ellipsometry systems [2] have been developed for measuring the physical properties of films of tilted smectic phases. Our null-transmission ellipsometry system draws from these designs. An improvement that we have made is to use the WPCSAWD path for the laser beam which minimizes the effect of the windows on the resolution of the system. In the usual polarizer–compensator–window–sample–window–analyser–detector configuration, the windows distort the ellipticity of the light before and

after the sample, giving a limit to the reproducibility of Δ and Ψ of approximately 0.01°. A discussion of this effect can be found in [1]. In our WPCSAWD arrangement both windows are outside the region in which the slight polarization distortions due to the windows matter. To our knowledge such an arrangement was first used in [3]. In our set-up the polarizer, compensator, and analyser are in the same sealed exchange gas environment as the sample. However, this exchange gas has to pass through small holes to travel between the oven and two chambers housing the polarizer, compensator and analyser. This allows us to keep the polarizer, compensator, and analyser at near room temperature while the sample temperature is elevated. Helium or argon is used as exchange gas, which keeps sample degradation to a minimum. For example, we have been able to study the somewhat unstable compound DOBAMBC† over a period of days with minimal observed change in the transition temperature. It is worth noting that the 3/4 atm. exchange gas eliminates the concerns usually present in high vacuum systems, such as contamination of the vacuum due to the rotation motors. One other solution to the problems caused by the windows is to remove the windows entirely, as has been done in one system. In this case a slow flow of inert gas reduces the influx of moisture or other contaminants. However, this arrangement does not isolate the sample environment as completely as our system.

We have found it necessary to control the temperature of the compensator to within 0.05°C in order to limit the drift in the compensator-induced phase lag of the light incident on the sample. The entire stage housing the compensator is held at 30.00°C using heating wire to provide heat, and a thermistor to monitor the temperature and provide feedback to a temperature controller.

The most important advance over previous ellipsometry systems is the ability to measure the ellipsometric parameters as a function of orientation of the c-director of the molecules within the film. A rotation of the molecules can occur as a result of either an applied rotatable electric field in the plane of the film, discussed below, or thermal fluctuations. In many phases of interest, the average molecular orientations in one layer are coupled to adjacent layers through interlayer interactions. For this reason, all of the molecules rotate together. The orientation of the molecules sets the orientation of the dielectric tensor, the properties of which can be measured by ellipsometry. If the film responds to the electric field, then Ψ and Δ can be plotted as functions of the electric field orientation, as well as Ψ versus Δ. If the film does not respond to the electric field, then the azimuthal orientation is not known and we can plot only Ψ versus Δ. Because the symmetry of the optical structure depends on the symmetry of the layer structure, this technique allows us to probe the symmetry of the layer structure. The 4×4 matrix method allows us to model and fit the optical parameters, as discussed in the Appendix.

The rotatable electric field is produced by eight equally spaced electrodes surrounding the circular hole in the glass cover slip upon which the film is suspended, see figure 2 (*a*). The electrodes are connected so that they appear to radiate from the centre of the hole. To create an approximately constant electric field near the centre of the film hole, the voltage of the electrodes is set using a cosine function:

$$V_m = A \cos\left[\frac{2\pi(m-1)}{M} - \alpha\right].$$

Here M is the number of electrodes, m is an index for the electrodes, and α sets the angle of the electric field. We define α to be the angle between the incidence plane of the laser and the electric field direction, see figure 2 (*b*). Simulations of the electric field in the plane of the film demonstrate its uniformity. Figure 2 (*a*) shows one such simulation for $\alpha = 0$. The simulation was done using the relaxation technique on a three-dimensional array. The electrodes were simulated as thin radial objects of known voltage. The simulation results show that near the centre of the hole the electric field orientation is good, although the field strength is smallest near the centre. If the film responds to an electric field, the orientation of the electric field sets the orientation of the molecules. The electric field used, typically on the order of 1 V cm^{-1}, is sufficient to align a net polarization but is much smaller than the critical field required to unwind the optical helix of a sample or to produce a mass flow in the film.

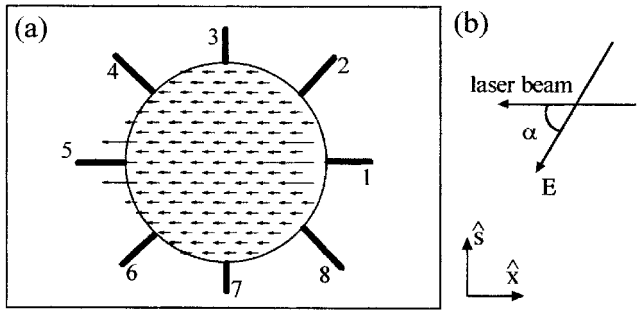

Figure 2. (*a*) A diagram of the film plate used with electrodes drawn as numbered lines. A simulation of the electric field at $\alpha = 0$ is shown with arrows, where the length corresponds to the magnitude of the field. (*b*) α, the angle between the electric field (**E**) and the incidence plane of the laser beam, is shown.

†DOBAMBC refers to *p*-decyloxybenzylidene-*p*-amino-2-methylbutyl cinnamate.

The polarization of each layer is typically assumed to be perpendicular to the tilt plane, and the net polarization is assumed to align parallel to the electric field. This assumption is altered if there is reason to believe that the polarization may lie along another direction, e.g. in the case with dominant flexoelectric contributions, the polarization would be (approximately) in the tilt plane.

3. Three applications of the technique

To simulate the data it is necessary to determine the indices of refraction [4]. These are found in the SmA phase, a smectic phase with the long axes of the molecules aligned along the layer normal. In SmA, Δ and Ψ depend on the index of refraction along the long axis of the molecule (n_e), the index of refraction perpendicular to this (n_o), the SmA layer spacing (d), and the number of smectic layers (N) in the film. Only two indices of refraction are used because the SmA phase is uniaxial. By measuring Ψ and Δ for a series of films in the SmA phase, these quantities can be determined by modelling the data using the simple structure for SmA described above. The values of n_o, n_e, and d determined from this method for DOBAMBC are $n_o = 1.4775 \pm 0.0005$, $n_e = 1.683 \pm 0.004$, and $d = 33.15 \pm 0.2$ Å at 110°C. For comparison, Garoff [5] found $n_o = 1.478 \pm 0.002$ and $n_e = 1.692 \pm 0.001$ at 110°C in a bulk sample using a modified Pulfrich critical-angle refractometer. The value of d is found to be 32.90 ± 0.05 Å at 110°C from X-ray diffraction using a rotating anode machine. Although the values found by null-transmission ellipsometry do not exactly match those found by other methods, in most circumstances we need only reasonable values for these optical parameters in order to determine the layer structure of most samples. As a check of the ellipsometry systems measurement, a calculation can be made of $(2n_o^2 + n_e^2)^{1/2} d$, which is a measure of the optical thickness. The value of this parameter found by ellipsometry divided by that measured by the other techniques is 1.005; this gives us confidence in our ability to measure the optical thickness. Using the parameters found, the thickness in a number of layers can be determined from the measured value of Ψ and Δ in the SmA phase. Upon cooling into the tilted phase the film thickness reduces due to the molecular tilt. However, the number of layers remains the same.

Three examples are given to demonstrate the unique capability of our ellipsometry system. The first example is chosen as it gives a measure of the resolution capabilities of the set-up and shows how information about the symmetry can be acquired. The second illustrates how information about the symmetry of a structure can be learned in a relatively clear-cut situation. Finally, the utility of this method in determining the molecular orientation in the surface layers is given in the third example.

3.1. *Symmetry of a one layer film in the B2 phase*

The B2 phase is of much experimental interest because it is an antiferroelectric liquid crystal phase formed by achiral bent-core molecules. The structure of the B2 phase has been determined [6], and a diagram of the structure found in films is shown in figure 3 (*a*). This is a tilted smectic phase, in which the molecular long axes are tilted away from the layer normal by an angle θ; in films, the tilt orientation is uniform throughout. Because of the shape of the molecules, a vector **b** can be defined which points along the bend of the molecule, see figure 3 (*b*). **b** can point in either direction perpendicular to the tilt plane, but within each layer **b** is uniform in a given domain. In films the orientation of **b** alternates from layer to layer. The net polarization (**P**) within each layer is determined to be parallel or antiparallel to **b**. The opening angle ϕ is also shown in figure 3 (*b*).

A film one-smectic-layer thick of the compound shown in figure 4 (*a*) has been studied [7]. The data collected at 80°C in the B2 phase are shown in figures 4 (*b*) and 4 (*c*) as crosses. It is clear from the data that the resolution in Ψ is about 0.002°; our resolution in Δ is more difficult to determine because Δ tends to depend more strongly on the tilt orientation of the film and shows a much larger variation. There are two possible structures for a one-layer film, as **b** has two possible orientations relative to the tilt orientation. This corresponds to two different possible handednesses for the chirality of the layer [6]. Both handednesses existed in the same film but formed different domains in the film, as could be observed from depolarized reflected light microscopy. To model the optical properties of a layer formed by bent-core molecules, it is typically sufficient to use a biaxial

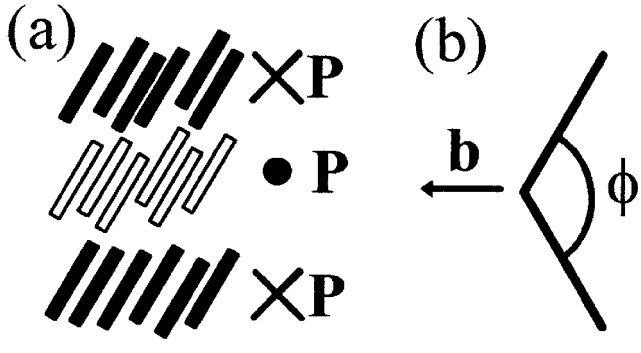

Figure 3. (*a*) The layer structure of the B2 phase found in films. Rectangles drawn solid represent molecules with **b** oriented into the page, while the open rectangles have **b** oriented out of the page. The polarization (**P**) is shown parallel to **b**, but may lie antiparallel to **b**. (*b*) A diagram of a single bent-core molecule; **b** lies along the bend of the molecule, and ϕ is the opening angle of the molecule.

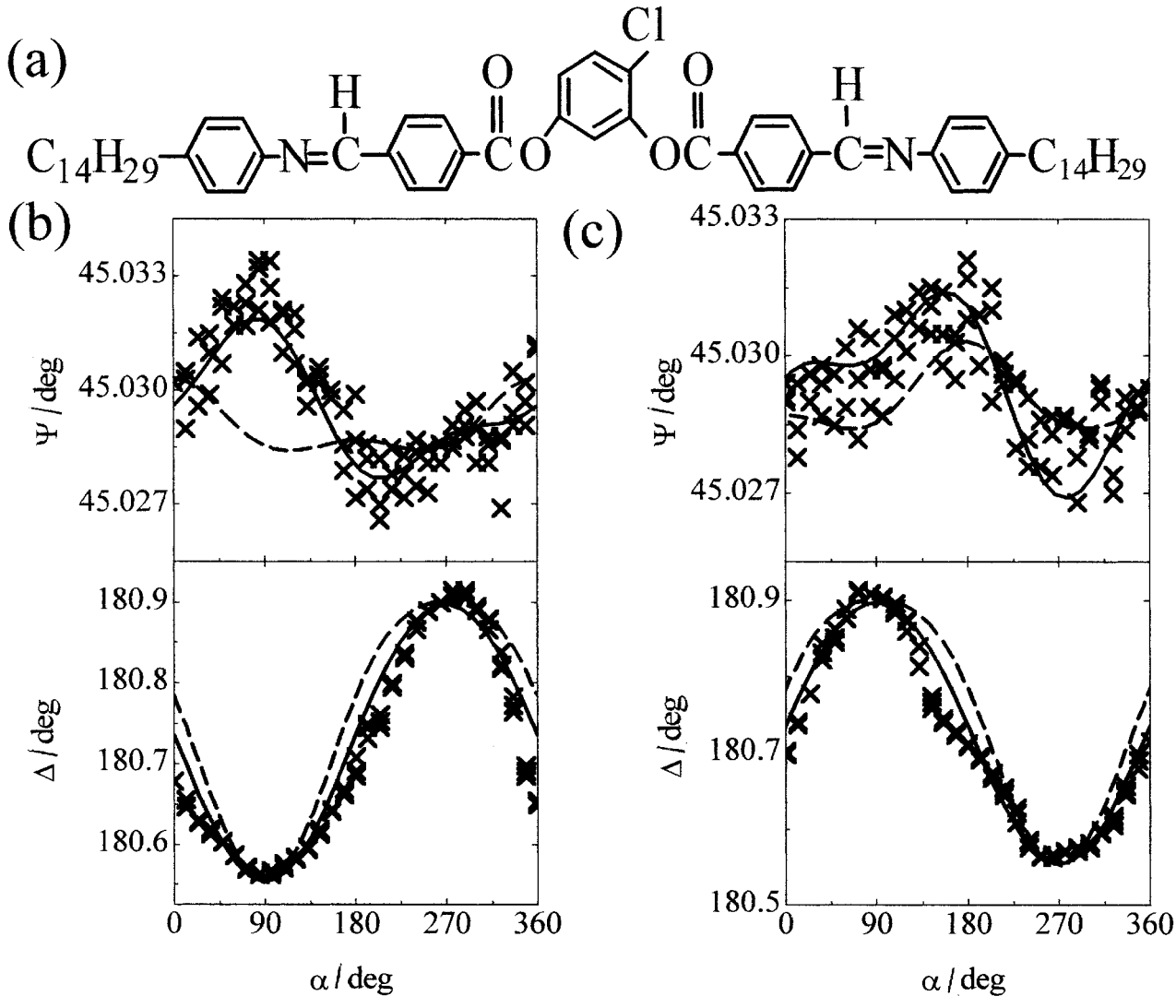

Figure 4. (*a*) The molecular structure of the bent-core molecule studied. (*b*) and (*c*) depict the data (crosses) and simulation (lines) of the two handednesses possible for a one-layer film. Simulations using a biaxial ellipsoid of refraction are drawn with dashed lines, while those made with a two-uniaxial-layers model are drawn as solid lines.

ellipsoid of refraction, shown with dashed lines; the best fit is shown. This model predicts data collected from both handednesses should be identical due to its symmetry. However, the data are different for the two handednesses.

For this reason an optical model in which the upper and lower half of the layer are each treated as a uniaxial slab was proposed. n_e is oriented along the leg of the molecule within that slab. By employing the 4×4 matrix technique, a best fit was made and is shown with solid lines. As can be seen, the model fits the data well. The optical parameters used in this simulation are $\theta = 30^\circ$, a smectic layer spacing of 49.4 Å, $n_o = 1.496$, $n_e = 1.710$, and $\phi = 127.2^\circ$. All these parameters are consistent with known values for bent-core molecules.

3.2. *Symmetry of the SmC^*_{FI2} phase*

The smectic antiferroelectric phase with a four-layer unit cell (SmC^*_{FI2}) has been studied by many approaches. This phase is one of the smectic C (SmC) variants that was discovered when liquid crystals with a high spontaneous polarization were synthesized. It is known that this phase is similar to SmC in that the molecules are tilted with respect to the layer normal by an angle θ and it forms smectic layers. In the smectic C* phase the tilt azimuth is uniformly oriented except for a long helical pitch of optical wavelengths.

In order to learn more about the SmC^*_{FI2} phase, numerous films of the compound shown in figure 5(*a*) were studied [8]. One important general feature found is that Δ and Ψ changed little upon rotating the electric

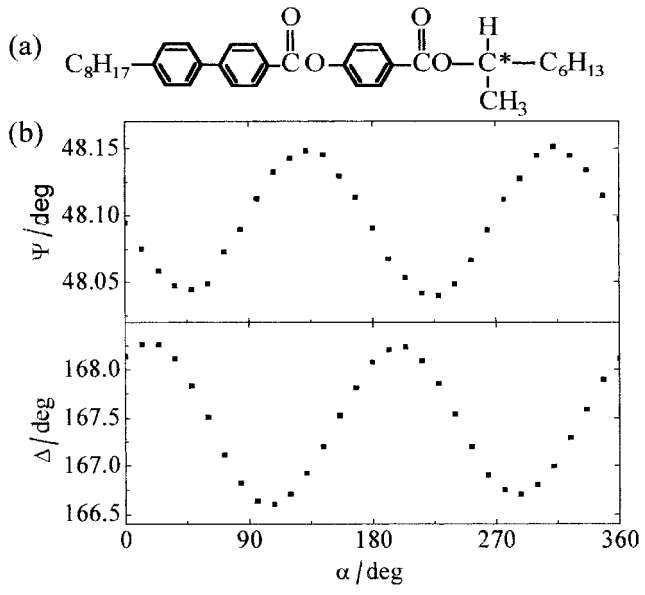

Figure 5. (*a*) The molecular diagram for the compound from which the data shown in (*b*) was taken. The film was 119-layers thick.

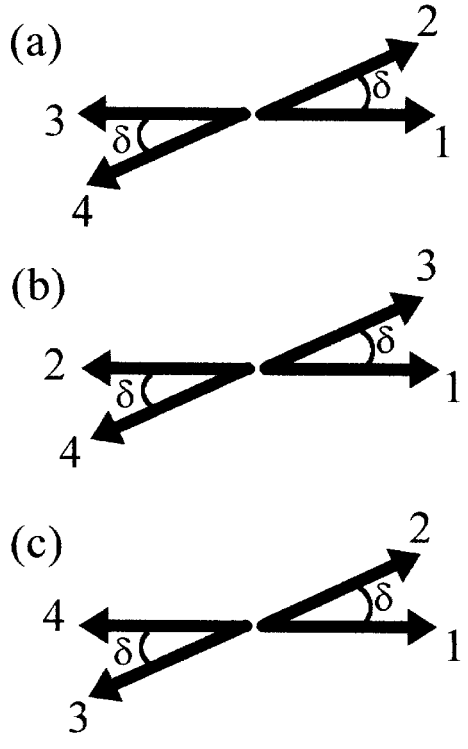

Figure 6. (*a–c*) The three possible structures allowed from the symmetry of the data with a four-layer unit cell. The arrows signify the orientation of the ^{c}-director of the ^{n}th layer of the unit cell, where ^{n} is the number written at the tip of the arrow. The angle δ measures the degree of distortion from an Ising-like state where the ^{c}-directors in all layers lie in a plane.

field by 180°, see figure 5 (*b*). This set of data was obtained from a 119 ± 1-layer film. The small deviation for 180° symmetry may be due to a different molecular arrangement at the surface of the film. This implied that the optical properties of the SmC^*_{F12} phase also changed little upon rotating the electric field by 180°. Both Ψ and Δ show a large variation as a function of α; this indicates a strong biaxiality of the phase. Thus this phase cannot be described by a simple four-layer helix. From resonant X-ray experiments, it has been determined that the unit cell of the structure is four-layers except for a long helical pitch, and that the structure is not well described by a simple Ising model (where the tilt orientations are confined to a plane). From these facts only three possible structures remained for the interlayer structure of this phase. The ^{c}-director of each layer in the unit cell for these structures is shown in figure 6. The distortion from an Ising model is described by an angle δ. The other 3 perturbations of the structure are the same as those shown except that $\delta > \pi/2$. Because of the long wavelength of the light (6328 Å) relative to the unit cell (≈160 Å), the difference between optical data collected from these structures is practically impossible to distinguish. Recent high resolution resonant X-ray experiments, prompted by our ellipsometry result, have determined that the structure shown in figure 6 (*a*) is correct [9].

3.3. *Determination of the surface structure of the SmC* phase of one compound*

Films provide a unique system for the examination of surface ordering. In liquid crystal films the air–film interface often favours the ordering characteristic of a lower temperature phase exhibited by the interior layers. If the structure of the interior layers is known, then an accurate determination can be made of the structure of the surface layers, as the following example illustrates.

One compound, with SmC^*_{F12} as the phase directly below SmC* was studied, as shown in figure 7 (*a*) [10]. It was observed that in the SmC* phase the number of surface layers increased upon approaching the SmC^*_{F12} phase, and appeared to diverge at the bulk transition temperature. The surface layers could be distinguished from the bulk because the orientation of the tilt azimuth at the surface alternated from layer to layer, but in the bulk the tilt was uniformly aligned except for a long helical pitch of about 80 layers. The number of surface layers was found to be irreproducible at some temperatures, and the top and bottom surfaces often exhibited a different number of surface layers. The number of surface layers was determined by simulating the film using a simple model. In the model, the interior layers have a simple helical structure, while the ^{c}-director rotates by 180° between adjacent layers for those layers counted as being part of

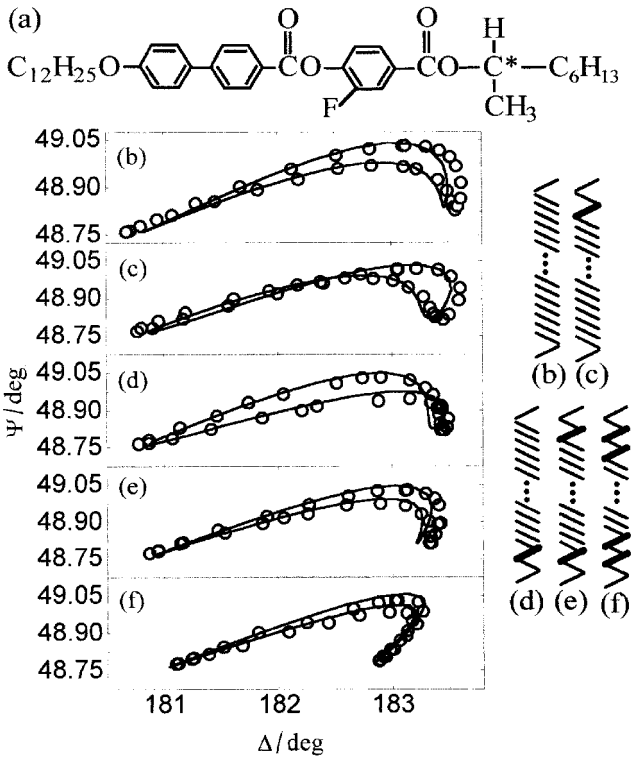

Figure 7. (*a*) The molecular diagram of the compound from which the data shown in (*b–f*) were taken. (*b–f*) data (circles) and simulations (lines) of 24-layer films in the SmC* phase. On the right is shown the molecular configuration used in the simulations. The data and simulations are described in detail in the text.

the surface. A number of films of different thicknesses were studied to determine the bulk parameters, i.e. the optical pitch and θ. The parameters n_o, n_e, and d were found in the SmA phase. The biaxiality in the molecular frame of the SmC* phase is ignored because it is expected to be very small.

The data from 24-layer films at 85.0°C, which is about 2.3 K above the SmC*–SmC^*_{F12} transition temperature, are shown as circles in figures 7(*b–f*). These data were collected by heating to the SmA phase and cooling to 85.0°C, repeatedly. The number of surface layers was found to be irreproducible. Five different structures were observed upon repeating this procedure a total of 10 times on two different films of the same thickness. The structure of the surface can be found because the Ψ versus Δ curve depends on the surface structure. Simulations of the data made with the structure shown on the right of the figure are shown with lines. The values used in this simulation are $n_o = 1.479$, $n_e = 1.610$, and $d = 37.9$ Å. A tilt angle θ of 22° was used. Here it is possible to determine the structure more easily than in the SmC^*_{F12} phase because the inversion of the azimuth of a single layer significantly changes the average local optical properties. The average local optical properties for the structures in figure 6 are practically indistinguishable.

4. Conclusion

A high resolution null-transmission ellipsometry system has been described where the ellipsometric parameters are measured with a resolution of 0.002°. This set-up has been developed for measurement of the optical properties of liquid crystal free-standing films in a sealed, temperature-controlled environment. The two most important features of this design were the removal of the windows from the portion of the beam path where they could affect the polarization state of the light, and the unique way in which data was collected as a function of electric field orientation. By using an applied electric field which can be reoriented within the plane of the film, the optical symmetry and molecular arrangements within free-standing liquid crystal films can be determined. The utility of our system has been demonstrated through three key examples. These three cases demonstrated the resolution of the system, showed how the symmetry of a phase can be inferred, and gave an example of how the surface structure can be obtained.

We would like to thank S. Pankratz, P. Mach, and Ch. Bahr for help in designing and constructing the experimental setup. This work was partially supported by the National Science Foundation, Solid State Chemistry Program under Grant No. DMR-9703898 and 0106122 and the NATO International Scientific Exchange Program.

Appendix

Calculation of Ψ and Δ

By using the 4 × 4 matrix method [11] to simulate the effect of the film on polarized light [12], we can determine the optical parameters of the film. The 4 × 4 matrix method is a matrix formulation of Maxwell's equations that makes the following assumptions about the sample: the optical properties of the sample change along only one direction, the incident light is a plane wave, and there are only linear optical effects. We add the following assumptions to describe approximately our free-standing films and simplify the calculations greatly: the sample can be divided into slabs corresponding to smectic layers where within each slab the optical properties are constant and the magnetic permeability is 1. This method is advantageous because it rewrites Maxwell's equations for the electric and magnetic fields as four coupled first order differential equations that can be formulated as a 4 × 4 transfer matrix. The propagation of the electromagnetic wave through the sample can be calculated by the transfer matrix. If each smectic layer is uniaxial, an exact solution exists for the transfer matrix [13]. If each layer is biaxial then the transfer matrix

can be found numerically. From the transfer matrix it is possible to calculate the 2×2-transmission matrix (T_{jk}) which relates the incident electric field components to the transmitted electric field components [1], where T is defined by the following equation:

$$\begin{bmatrix} E_{pt} \\ E_{st} \end{bmatrix} = \begin{bmatrix} T_{11} & T_{12} \\ T_{21} & T_{22} \end{bmatrix} \begin{bmatrix} E_{pi} \\ E_{si} \end{bmatrix}.$$

Here E_{pi}, E_{si}, E_{pt} and E_{st} are the p and s components of the incident and transmitted light.

Δ and Ψ can be calculated from the transmission matrix. The effect of the polarizer and compensator in our configuration is to create elliptically polarized light with p-component and s-components equal to 1 and $\exp(i\Delta)$, respectively. The analyser is rotated at an angle Ψ from the p axis. Because we are assuming that all of the optical components are ideal, it is possible in this configuration to create zero transmitted light with the proper angles of the polarizer and analyser. For a null to occur, the light emerging from the sample must be linearly polarized. This implies that $\mathrm{Im}[(T_{11} + T_{12}\exp(i\Delta))/(T_{21} + T_{22}\exp(i\Delta))] = 0$. This equation can be solved exactly for Δ. The following is the solution:

$$\Delta = \arg(T_{11}T_{22}^{*} - T_{12}^{*}T_{21}) + \arcsin\left(\frac{\mathrm{Im}(T_{11}T_{21}^{*} - T_{12}^{*}T_{22})}{|T_{11}T_{22}^{*} - T_{12}^{*}T_{21}|}\right).$$

The angle to the p axis of the light after the sample is given by $\arctan[(T_{21} + T_{22}\exp(i\Delta))/(T_{11} + T_{12}\exp(i\Delta))]$. Ψ should then be set at 90° to this angle to produce a null signal, i.e.

$$\Psi = \arctan\left(\frac{T_{21} + T_{22}\exp(i\Delta)}{T_{11} + T_{12}\exp(i\Delta)}\right) \pm \frac{\pi}{2}.$$

These equations for Δ and Ψ assume perfect optical components. If the optical components are imperfect then Δ and Ψ must be found numerically.

References

[1] Azzam, R. M. A., and Bashara, N. M., 1989, *Ellipsometry and Polarized Light* (Amsterdam: North-Holland).

[2] Heinekamp, S., Pelcovitis, R. A., Fontes, E., Chen, E. Y., Pindak, R., and Meyer, R. B., 1984, *Phys. Rev. Lett.*, **52,** 1017; Amador, S. M., and Pershan, P. S., 1990, *Phys. Rev. A*, **41,** 4326; Bahr, Ch. and Fliegner, D., 1992, *Phys. Rev. A*, **46,** 7657.

[3] Yamamoto, M., and Heavens, O. S., 1980, *Surf. Sci.*, **96,** 202.

[4] Olson, D. A., Pankratz, S., Johnson, P. M., Cady, A., Nguyen, H. T., and Huang, C. C., 2001, *Phys. Rev. E*, **63,** 061711.

[5] Garoff, S., 1977, PhD thesis, Harvard University, Cambridge, Mass., USA.

[6] Link, D. R., Natale, G., Shao, R., Maclennan, J. E., Clark, N. A., Körblova, E., and Walba, D. M., 1997, *Science*, **278,** 1924.

[7] Olson, D. A., Cady, A., Weissflog, W., Nguyen, H. T., and Huang, C. C., 2001, *Phys. Rev. E*, **64,** 051713.

[8] Johnson, P. M., Olson, D. A., Pankratz, S., Nguyen, T., Goodby, J., Hird, M., and Huang, C. C., 2000, *Phys. Rev. Lett.*, **84,** 4870.

[9] Cady, A., Pitney, J. A., Pindak, R., Matkin, L. S., Watson, S. J., Gleeson, H. F., Cluzeau, P., Barois, P., Levelut, A.-M., Caliebe, W., Goodby, J. W., Hird, M., and Huang, C. C., 2001, *Phys. Rev. E*, **64,** 050702.

[10] Han, X. F., Olson, D. A., Cady, A., Goodby, J. W., and Huang, C. C., 2002, *Phys. Rev. E*, **65,** 010704.

[11] Berreman, D. W., 1972, *J. Opt. Soc. Am.*, **62,** 502.

[12] Schlauf, D., Bahr, Ch., Dolganov, V. K., and Goodby, J. W., 1999, *Eur. Phys. J. B*, **9,** 461.

[13] Wöhler, H., Haas, G., Fritsch, M., and Mlynski, D. A., 1988, *J. Opt. Soc. Am. A*, **5,** 1554.